Segment Orientation in a Quiescent Block Copolymer Melt Studied by Raman Scattering

Lynden A. Archer* and Gerald G. Fuller

Department of Chemical Engineering, Stanford University, Stanford, California 94305-5025

*Received November 15, 1993; Revised Manuscript Received May 4, 1994**

ABSTRACT: Segment orientation of a poly(styrene)–poly(butadiene) star diblock copolymer melt is investigated using polarization-modulated laser Raman scattering (PMLRS). The PMLRS technique is based on Raman spectroscopy and allows for the simultaneous measurement of statistical segment orientation and birefringence. It is found that at temperatures below the glass transition temperature of poly(styrene), segments in both poly(styrene) and poly(butadiene) blocks preferentially align normal to the interface separating microdomains. However, at temperatures greater than the glass transition temperature of poly(styrene), segment orientation disappears. At this temperature, a dramatic decrease in birefringence is also observed. The implications of these findings on the existence of copolymer chain extension in the so-called strong segregation limit are discussed.

1. Introduction

Block copolymers are macromolecules created by covalently joining two chemically distinct polymer units (blocks) into one molecule. If the blocks are immiscible, they attempt to separate. However, because of their connectivity, the length scale on which phase separation can occur is restricted. This results in the formation of microdomains richer in one species and separated by distances on the order of the copolymer's radius of gyration. The connectivity of individual units also places restrictions on molecular conformations and, therefore, results in a loss of conformational entropy. The balance between the enthalpic penalty for mixing and the entropy loss resulting from phase separation determines the phase behavior of block copolymers. At temperatures exceeding the microphase separation temperature (MST), this balance favors mixing while, at lower temperatures, microphase separation occurs. Above the MST, in the so-called weak segregation limit (WSL), interactions between units of opposite type are weak and chain configurations are unperturbed by block connectivity; thus, Gaussian chain statistics are expected to apply. On the other hand, at temperatures well below the MST, in the so-called strong segregation limit (SSL), interactions are strengthened and interspecies contact at the interface separating microphases is minimal. Incompressibility of block copolymer melts imposes a uniform space filling requirement that further restricts the number of admissible molecular conformations. The net effect is that in the SSL molecular strands orient and are perhaps stretched normal to the interface separating microdomains. Under conditions of strong chain stretching, a departure from Gaussian chain statistics is expected.[1]

Recently, following the initial work of Semenov,[2] interest in the role of chain stretching in the SSL has been increasing. Semenov assumed strong chain extension occurs in the SSL, and showed that the presence of such stretching considerably simplifies the description of block copolymer statistical thermodynamics in the SSL. In a recent study, Almadal et al.[3] used neutron scattering measurements to study coil dimensions in a diblock copolymer and reported chain stretching well into the homogeneous phase. These authors were also able to identify a crossover from Gaussian to stretched-coil chain configurations above the MST. Subsequently Lodge et al.[4] used a Kuhn–Grun type analysis to determine the intrinsic birefringence resulting from chain stretch and orientation for quiescent assemblies of tethered chains. These authors showed that even under circumstances of moderate chain stretch, alignment of segment vectors normal to the interface separating microdomains may result in intrinsic birefringences of quiescent block copolymer melts being of the same order of magnitude as form birefringence. This result appears to contradict previous birefringence measurements on single crystal poly(styrene)–poly(butadiene) (PS–PBD) triblock copolymers, wherein it was found that the measured birefringence was predominantly form birefringence.[5]

In this study we adopt an alternative approach to investigating polymer chain stretch in the SSL. Instead of considering changes in the absolute dimension of polymer strands, we concern ourselves with the orientation of statistical polymer segments constituting such strands. As pointed out earlier, segment orientation normal to the interface separating microdomains results from a loss of configurational entropy produced by the dual restrictions of block connectivity and localization of junction points at the interface separating microdomains. It is therefore expected to precede chain stretch. Indeed, it may be argued that whenever polymer chain stretch becomes important, segmental orientation should be well developed. Thus, measurement of molecular segment orientation for quiescent, microphase-separated block copolymer melts provides an alternative means for studying the factors affecting chain extension in the SSL.

In this work we use a spectroscopic experimental technique, polarization-modulated laser Raman scattering (PMLRS), to study segment orientation. Due to its spectroscopic character, this method affords the unique opportunity of targeting specific structural units for study. In addition, it allows for the measurement of both the second and fourth moments of the orientation distribution of segment vectors. For a very sharply peaked distribution function, resulting from strong segment orientation about a given direction, the fourth moment is simply the square of the second. However, for a random distribution, resulting from poor segment orientation, the fourth moment is related to the square of the second moment by a constant factor of 1.8. Thus, when this ratio is monitored, the extent to which polymer segments are oriented in each block can be assessed. In particular we consider the effect of temperature on the segmental orientation of a single

* Abstract published in *Advance ACS Abstracts*, June 1, 1994.

0024-9297/94/2227-4359$04.50/0

crystal PS–PBD multiarm star diblock copolymer melt. The star architecture is believed to be particularly well suited for investigating the forces fostering segment alignment and chain extension. The topological constraint of the central junction point of a star places severe restrictions on accessible chain conformations and should, therefore, promote segment alignment and chain extension.

2. Experiment

2.1. Sample Preparation. The sample used in this study is a PS–PBD six-arm star diblock copolymer. This polymer is a research-grade material provided by the Shell Development Co. and has an arm molecular weight of 27 800 (GPC), polydispersity index, $(\bar{M}_w/\bar{M}_n)|_{arm}$, of 1.3, and styrene content of 30 weight %. In this material, the inner region of the PS–PBD star consists of PBD units.

Film specimens approximately 0.3 mm thick were prepared by solvent casting from a 10 weight % toluene solution which contained 1% Irganox 1010 antioxidant (Cieba Geigy Corp.). Solvent casting was performed at 50 °C using a slow evaporation technique, lasting for a period of 2 weeks. Films thus prepared were further dried under vacuum at a temperature of 90 °C for 48 h and then annealed, under a constant load, at a temperature of 120 °C for a period of 6 h. The presence of the load during annealing causes radial alignment of the microdomains and results in the formation of uniformly birefringent sections (approximately 4 mm × 24 mm). Electron microscopy indicated that the microstructure of this material consisted of PS cylinders in a PBD matrix. Static birefringence and dynamic mechanical rheometry measurements indicated that this material disorders at a temperature between 145 and 149 °C. In the mechanical experiments, the appearance of anomalous low-frequency behavior of the loss (G'') and storage (G') moduli were interpreted to be evidence for the onset of microphase separation.

2.2. Raman Scattering. A detailed description of the PMLRS experimental technique has been presented elsewhere.[6-8] Briefly, Raman scattering arises from the interaction between radiation induced oscillating electric dipoles and molecular vibration modes. This interaction yields radiation shifted in wavelength relative to the excitation wavelength. The magnitude of the wavelength shift depends on the functional groups participating in the vibration mode, and thus Raman scattering, like infrared absorption, is a vibrational spectroscopy. Furthermore, because of differences in the symmetries of the transition moments for Raman scattering and infrared absorption, vibration modes such as the carbon–carbon symmetric stretch, localized in the backbone of a polymer chain, that are inactive for infrared absorption, are active for Raman scattering.[7,9,10] This gives Raman scattering certain advantages over infrared absorption spectroscopy for studying segmental orientation in polymer strands.

It is possible to describe an individual Raman scattering event by a second rank tensor, the Raman tensor α'_{ij}.[9] This tensor can be shown to be related to the segment orientation vector, u_j, as follows:

$$\alpha_{ij} = \eta(\delta_{ij} + \hat{\epsilon}u_i u_j) \tag{1}$$

where $\eta = \alpha_1 + (A/2)$, $\hat{\epsilon} = (B - (A/2))/(\alpha_1 + (A/2))$, $A = (\alpha_2 - \alpha_1)\cos^2\rho_0 + (\alpha_3 - \alpha_1)\sin^2\rho_0$, and $B = (\alpha_2 - \alpha_1)\sin^2\rho_0 + (\alpha_3 - \alpha_1)\cos^2\rho_0$. Here, α_1, α_2, and α_3 are the principal values of the Raman tensor expressed in a principal coordinate system coincident with a Raman vibration mode, and ρ_0 is the angle between the long axis of a molecular segment (assumed here to be cylindrically symmetric) and one of the principal axes of the Raman tensor characterizing the vibration mode of interest. Equation 1 can be shown to be part of a more general result and is obtained by preaveraging a microscopic Raman tensor.[7,8]

An experimental arrangement for performing Raman scattering measurements is presented elsewhere.[6] This arrangement provides simultaneous measurement of forward Raman scattering and birefringence. The modulated Raman scattered intensity at a given scattered wavelength can be shown to be of the form

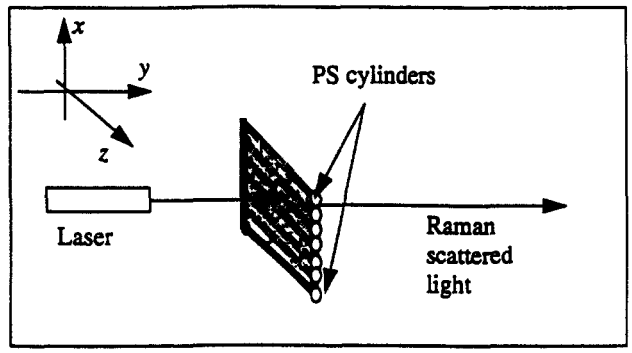

Figure 1. Schematic showing cylinder orientation and experimental geometry.

$$\frac{I_s(t)}{I_0} = I_{dc} + 2J_2(A)I_{2\omega}\cos(2\omega t) + 2J_1(A)I_\omega \sin(\omega t) \tag{2}$$

where ω is the modulation frequency, $J_i(A)$ are Bessel function coefficients resulting from modulation, I_0 is a constant that depends on the incident light intensity and instrumental factors and the Fourier amplitudes, and I_{dc}, $I_{2\omega}$, and I_ω are experimental measurables that are recovered using low-pass filters and lock-in amplifiers.

In this experiment, laser light propagates in the y-direction (Figure 1), and forward Raman scattered radiation with polarization vectors in the x–z plane is collected. Block copolymer monodomain samples are placed such that the z-axis of the laboratory coordinate frame is parallel to the long axis of the PS cylinders, and therefore perpendicular to the interface separating the PS and PBD domains (perpendicular to the direction of preferential segmental alignment). The x-direction is taken to be the direction of preferential segment alignment.

For this arrangement, experimental measurables are related to the Raman tensor elements and the birefringence retardation as follows:[7,8]

$$I_{dc} = \frac{1}{2}\langle \alpha_{xx}^2 + \alpha'^2_{zz} + 2\alpha'^2_{xz}\rangle \tag{3}$$

$$I_{2\omega} = \frac{1}{2}\langle \alpha'^2_{xx} - \alpha'^2_{zz}\rangle \tag{4}$$

$$I_\omega = \langle \alpha'_{xx}\alpha'_{zz}\rangle S\left(\frac{\beta\delta'}{2}\right)\sin\left\{\delta'\left(1-\frac{\beta}{2}\right)\right\} - \langle \alpha'^2_{xz}\rangle \sin\left(\frac{\beta\delta'}{2}\right)S\left\{\delta'\left(1-\frac{\beta}{2}\right)\right\} \tag{5}$$

where the angular brackets signify that quantities are averaged over a distribution of segment orientations and δ' is the birefringence retardation and is related to the birefringence, $\Delta n'$, by $\delta' = (2\pi\Delta n d)/\lambda_0$, where d is the sample thickness, λ_0 is the excitation wavelength, and $S(x) = \sin(x)/x$, $\beta = (\lambda_s - \lambda_0)/\lambda_s$, where λ_s is the wavelength of Raman scattered light. The parameter β is a small number for the vibrations of interest in this work. This permits us to rewrite eq 5 as

$$I_\omega = \langle \alpha'_{xx}\alpha'_{zz}\rangle \sin\delta' \tag{6}$$

If eq 1 is substituted into eqs 3, 4, and 6, the Raman measurables are all found to be linearly dependent on the second and fourth moments of the segment distribution. In particular, $I_{2\omega}$ is equal to a linear combination of the anisotropies in the second and fourth moments and vanishes for an isotropic distribution of segments. This quantity is analogous to infrared dichroism. Unlike dichroism, which measures anisotropy in only the second moment, $I_{2\omega}$ measures anisotropy in both the second and fourth moments of the orientation distribution of segment vectors.

3. Results and Discussion

Repeat units for PS and PBD blocks showing the Raman active vibration modes of interest for this work are presented in Figure 2a,b, respectively. A Raman spectrum of this material is presented in Figure 3. The Raman scattering peak at 1029 cm^{-1} is characteristic of the C—C

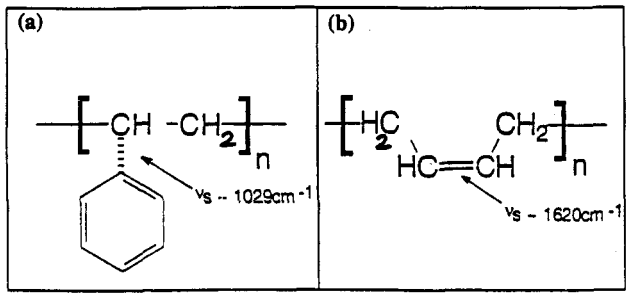

Figure 2. (a), (b) PS and PBD repeat units showing vibration modes of interest.

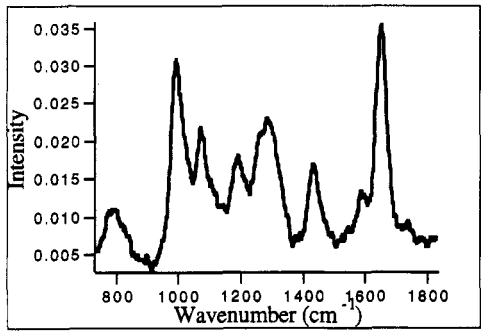

Figure 3. Raman spectrum of the PS–PBD block copolymer.

aromatic–aliphatic stretching vibration which, for this copolymer, is unique to the PS block. On the other hand, the peak at 1620 cm^{-1} is assigned to the C=C symmetric stretching vibration mode and results from the PBD units present in the specimen. These Raman peaks are well separated and, therefore, may be used to determine the orientation of polymer strands comprising each individual block of a PS–PBD block copolymer.

Modulated Raman spectra and birefringence are presented as a function of temperature in Figure 4a,d (spectra are shifted vertically for clarity of presentation). The angle χ appearing in Figure 4d is measured from the x-axis and describes the orientation of the birefringence, $\Delta n'$, with respect to this axis. Here we have arbitrarily defined $\Delta n'$ with respect to the x-axis; therefore, for the experimental geometry used here, $\chi = 90°$ for form birefringence, due to the orientation of PS cylinders along the z-axis, and $\chi = 0°$ for intrinsic birefringence, due to the fact that segments orient normal to the interface separating the domains, i.e. along the x-axis.

These results can be used to compute anisotropies in the second and fourth moments for the PS and PBD units using the following relations:

$$\langle u_x^2 - u_z^2 \rangle = \frac{15 - 15r_1 - 33r_2 + \hat{\epsilon}(10 - 10r_1 - 22r_2) + \hat{\epsilon}^2(1 - 4r_1 - 7r_2)}{\hat{\epsilon}(-29 - 4r_1 + 11r_2 - \hat{\epsilon}(11 + r_1 - 5r_2))} \quad (7)$$

$$\langle u_x^4 - u_z^4 \rangle = \frac{30 - 30r_1 + \hat{\epsilon}(20 - 20r_1 + 24r_2) + 2\hat{\epsilon}^2(1 - 4r_1 + 9r_2) + 6r_2\hat{\epsilon}^3}{\hat{\epsilon}^2(-29 - 4r_1 + 11r_2 - \hat{\epsilon}(11 + r_1 - 5r_2))} \quad (8)$$

where $r_1 = (I_\omega/\sin\delta)/I_{dc}$, $r_2 = I_{2\omega}/I_{dc}$, and $\hat{\epsilon}$ is a molecular parameter that can be determined from Raman scattering measurements on an isotropic sample.[7,8] $\sin\delta$ is obtained from the simultaneous birefringence measurement, and r_1 and r_2 are determined from the peak heights of the respective Fourier components of the Raman scattered intensity (Figure 4a–c).

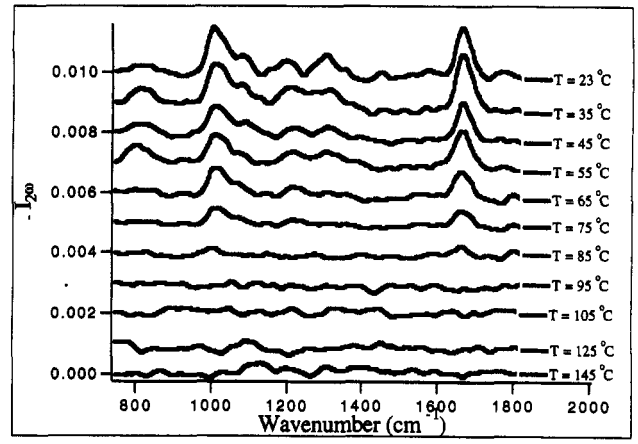

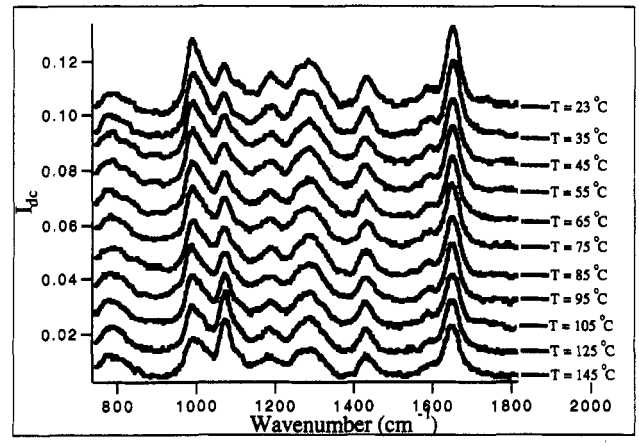

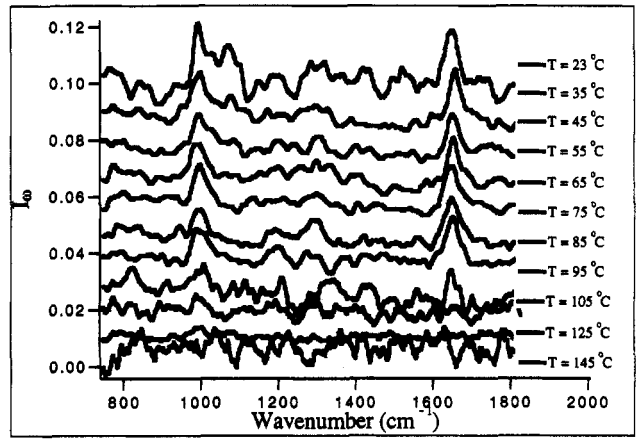

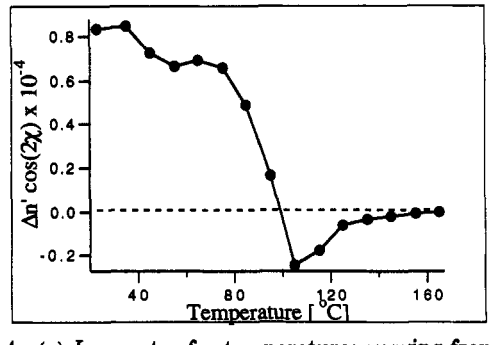

Figure 4. (a) $I_{2\omega}$ spectra for temperatures varying from 23 to 145 °C. (b) I_{dc} spectra for temperatures varying from 23 to 145 °C. (c) I_ω spectra for temperatures varying from 23 to 145 °C. (d) Birefringence of the PS–PBD block copolymer vs temperature. χ is measured with respect to the x-axis. It is 0° for intrinsic birefringence and 90° for form birefringence, due to the orientation of the PS cylinders (Figure 1).

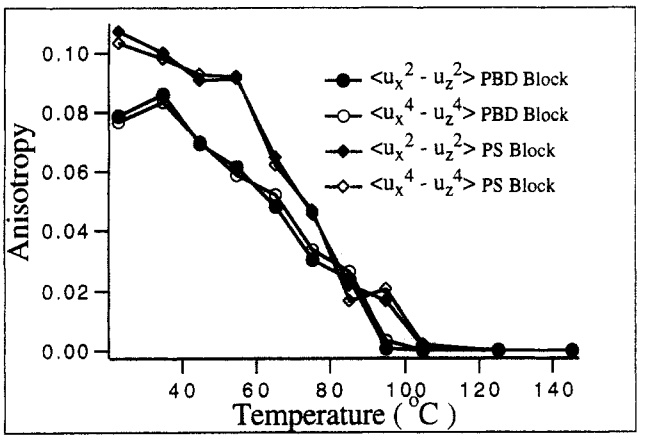

Figure 5. Anisotropies in the second and fourth moments vs temperature for poly(styrene) and poly(butadiene) chain segments.

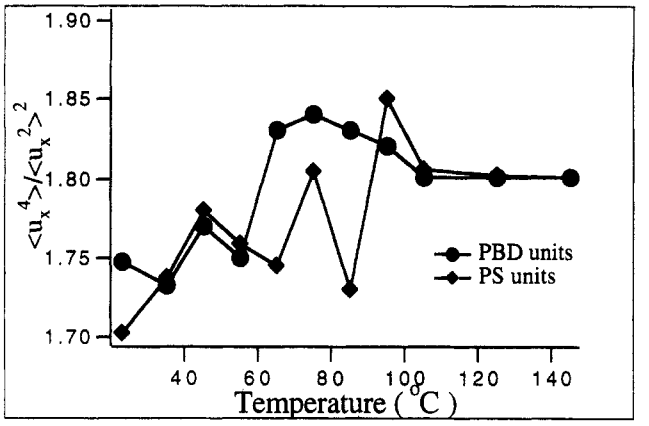

Figure 6. Ratio of the fourth moment to the square of the second vs temperature, for poly(styrene) and poly(butadiene) chain segments.

Anisotropies in moments calculated using eqs 7 and 8 are presented for various temperatures in Figure 5. These results show that at temperatures below 95 °C (the glass transition temperature of the PS units) PS and PBD segments are preferentially oriented normal to the interface separating the PS and PBD domains. At 95 °C segmental orientation disappears. This disappearance is rather gradual and is also apparent from Figure 4a, wherein the Raman scattering measurement of orientation anisotropy ($I_{2\omega}$) vanishes for both the C—C aromatic–aliphatic stretch and the C=C symmetric stretch vibrations. It is also apparent that the magnitude of the birefringence (Figure 4d) decreases rather dramatically at this point. In fact, this decrease is significantly more pronounced than the rate of disappearance of the birefringence at the MST and is consistent with the sharp drop in segment alignment (and thus intrinsic birefringence) observed from the Raman scattering measurements.

A more detailed analysis of Figure 5 reveals that at all temperatures PS segments are more oriented than PBD segments and that the decrease in orientation of PBD segments with increasing temperature very closely follows the decrease in orientation of PS segments. However, in either case, the decrease displays a much stronger temperature scaling than the $\chi^{-1/2}$ scaling of the interface width predicted by SSL theories[2,11] and presumably results from reorganization of domains. Here χ is the Flory–Huggins interaction parameter and, for this material, is given by $\chi = 0.0181 + 3.540/T$,[7] where T is the absolute temperature. Similar temperature scalings are observed for the birefringence of block copolymer liquids.[12]

The physical picture that emerges from these observations is that segmental orientation of PS and PBD blocks results from microphase separation. The coupling observed in the segment orientation of PS and PBD units perhaps indicates that preferential alignment of PBD segments perpendicular to the interface separating the PS and PBD domains is observed only because PS segments are preferentially aligned. Moreover, if these measurements are repeated after quenching the disordered material below $T_{g,PS}$, segment orientation normal to the interface separating PS and PBD microdomains is observed to reappear, and the Raman and birefringence signal ratios are also observed to approach their previous values after a period of several hours. Subsequent heating of the material through $T_{g,PS}$ results, as before, in the disappearance of segment orientation at $T_{g,PS}$. The reversibility of these measurements rules out frozen-in stresses as the source of PS and PBD segment alignment in this material. Instead, as stated earlier, we believe that such alignment results from microphase separation.

A plausible explanation for the disappearance of segmental orientation in the present material at $T_{g,PS}$ is found in the enhanced mobility of PS units above $T_{g,PS}$. Once PS strands are sufficiently mobile, copolymer chains can sample more configurations. Chain configurations that maximize configurational entropy are ultimately selected, thus reducing the probability of chains adopting configurations that result in chain extension and segmental orientation. Indeed, it might be argued that any chain stretching that might arise from instantaneous molecular conformations that produce such stretching is relaxed away very rapidly above $T_{g,PS}$. These observations appear to indicate that for the present material, the glass transition temperature of the block with the higher T_g divides the SSL into two regimes: one which occurs at temperatures below the glass transition temperature of the component with the higher T_g that is characterized by orientation and, perhaps, extension of polymer strands normal to the interface separating the domains, and another at temperatures above T_g, but lower than the MST, in which equilibrium chain configurations that do not produce such alignment are favored. Work is currently underway to investigate further the influence of the glass transition temperature on segment alignment in other block copolymer architectures.

To proceed, we next analyze the extent to which PS and PBD strands are oriented at temperatures below $T_{g,PS}$. This analysis rests on the evaluation of the ratio of the fourth moment to the square of the second moment of the distribution of segment vectors, $\langle u_x^4\rangle/\langle u_x^2\rangle$.[2] This ratio is presented in Figure 6. As pointed out earlier, it measures the shape of the orientation distribution function and, therefore, can be used to assess the strength of segment alignment in PS and PBD domains for the present block copolymer. It is apparent that at the lower temperatures $\langle u_x^4\rangle/\langle u_x^2\rangle^2$ is slightly lower than 1.8 (its value for a random distribution of segment vectors). This indicates that segment alignment is only moderately developed for this material and that polymer strands should obey Gaussian statistics. At temperatures as much as 30 deg below $T_{g,PS}$ this ratio fluctuates about a value of 1.8, indicating that the shape distribution of segment vectors is close to isotropic. At temperatures exceeding $T_{g,PS}$, this ratio is equal to 1.8, which demonstrates that the distribution of strand vectors is Gaussian.

Using the expression presented above for χ, the value of χN is estimated to be 13.2 at 23 °C, the lowest temperature studied. Here N is the total number of

Table 1. Physical Constants Used in Evaluating the Intrinsic Birefringence of the PS–PBD Block Copolymer Using Second Moment Anisotropies Determined from Raman Scattering Measurements

	n	ϕ	ρ, g cm^{-3}	$(\gamma_{i\parallel} - \gamma_{i\perp}) \times 10^{-25}$, cm^3
PS	1.59	0.27	1.05	+1.89
PBD	1.52	0.73	0.90	+80.0

monomer units per arm and has a value of approximately 440 for the present PS–PBD star diblock copolymer. The value of χN at the MST may be similarly estimated to be 11.7. Rubinstein and Obukhov[15] have shown that for diblock copolymers with $\chi N|_{MST} = 10.5$, chain stretch only becomes appreciable for values of χN in excess of 100. Therefore, the presence of only moderate segmental alignment in the present block copolymer melt is to some extent understandable.

Finally, we attempt to estimate the relative magnitude of intrinsic form birefringence of our PS–PBD copolymer. Form birefringence resulting from an array of cylinders with refractive index n_A, immersed in a medium with refractive index n_B, can be estimated by the following expression:[13]

$$\Delta n_f = [\phi_A n_A^2 + \phi_B n_B^2]^{0.5} - n_B\left[\frac{(1+\phi_A)n_A^2 + \phi_B n_B^2}{(1+\phi_B)n_B^2 + \phi_B n_A^2}\right]^{0.5} \quad (9)$$

where ϕ_A and ϕ_B are the volume fractions of species A and B. For PS cylinders immersed in a PBD matrix, $n_A \cong 1.59$, $n_B \cong 1.52$, $\phi_A = 0.27$, and $\phi_B = 0.73$ for the material used in thus work. With these values eq 9 yields $\Delta n_f = 6.01 \times 10^{-4}$. In our birefringence experiment PS cylinders are oriented perpendicular to the x-direction, the direction with respect to which the birefringence is defined. Thus, in Figure 4d, $\chi = 90°$ and the form contribution to the overall birefringence is $6.01 \times 10^{-4} \cos(90{\cdot}2) = -6.01 \times 10^{-4}$. Therefore, at a temperature of, e.g., 35 °C, this would imply an intrinsic contribution of approximately $+6.81 \times 10^{-4}$, which is of comparable magnitude to the estimated form birefringence.

The calculation of the intrinsic birefringence using the second moment anisotropies of PS and PBD segments rests on the simplistic assumption that the overall intrinsic birefringence of a block copolymer melt is the weighed sum of the birefringence of individual blocks. That is,

$$\Delta n_T = \varphi_{PS} f_{PS} \Delta n^0_{PS} + \varphi_{PBD} f_{PBD} \Delta n^0_{PBL} \quad (10)$$

where Δn_T is the net intrinsic birefringence, $\Delta n_i^0 = [2\pi(n_i^2 + 2)^2/9n_i](\gamma_{i\parallel} - \gamma_{i\perp})$, n_i is the refractive index of species i, $\gamma_{i\parallel}$ and $\gamma_{i\perp}$ are the pure component segment polarizabilities parallel and perpendicular to the long segment axis, $\varphi_i = \phi_i \rho_i N_A / M_i$ are the respective segment densities, and f_i are the second moment anisotropies of the respective blocks. Here, ρ_i is the density of species i, ϕ_i is the volume fraction of species i, N_A is the Avogadro number, and M_i is the molecular weight of species i. The values of these parameters used in determining the intrinsic birefringence are presented in Table 1. Using these parameters, the intrinsic birefringence at 35 °C is determined to be 1.5×10^{-4}, which is of the correct sign but is about 4 times smaller than its estimated value of $+6.81 \times 10^{-4}$.

Here it should be pointed out that because the stress-optical coefficient of PS is positive at temperatures below its glass transition temperature, the contributions of PS and PBD blocks to the overall intrinsic birefringence are both positive.[14] Below $T_{g,PS}$, the stress-optical coefficient of PS is about 2 orders of magnitude smaller than the stress-optical coefficient of PBD. This implies that the measured intrinsic birefringence results almost exclusively from the orientation of the PBD segments.

The above calculation is obviously only very approximate, but nevertheless it still shows that, at temperatures below $T_{g,PS}$, the intrinsic birefringence of the PS–PBD star diblock copolymer used in this study is of the same order of magnitude as the form birefringence. This is an important result since it indicates that even modest segment alignment can result in the observation of high intrinsic birefringences in block copolymer melts; which is in accord with the calculation of Lodge et al.[4] for simpler copolymer architectures.

4. Conclusions

In this study, a novel spectroscopic technique, PMLRS, was used to investigate segmental orientation in a PS–PBD six-arm star diblock copolymer at temperatures below the MST. This method allows for the simultaneous characterization of segment orientation in both blocks. We conclude that, at temperatures below the glass transition temperature of PS unit, both PS and PBD strands are oriented normal to the interface separating the PS and PBD domains. At higher temperatures segmental alignment disappears. We also conclude that the kinetics of polymer strand reorientation plays a crucial role in determining whether segment alignment and chain extension occur in the present quiescent block copolymer melt. We speculate that the glass transition temperature of the component with the higher T_g may divide the strong segregation limit into two regions: one in which segment alignment and chain extension are important, and another in which they are not.

Acknowledgment. We are grateful to the Shell Development Co. for providing the poly(styrene)–poly(butadiene) block copolymer melt used in this work. This study was supported by the National Science Foundation through Grant No. DMR 9120360.

References and Notes

(1) Bates, F. S.; Fredrickson, G. H. *Annu. Rev. Phys. Chem.* **1990**, *41*, 525.
(2) Semenov, A. N. *Sov. Phys. JETP* **1985**, *61* (4), 732.
(3) Almdal, K.; Rosedale, J. H.; Bates, F. S.; Wignall, G. D.; Fredrickson, G. H. *Phys. Rev. Lett.* **1990**, *9*, 1112.
(4) Lodge, T. P.; Fredrickson, G. H. *Macromolecules* **1992**, *25*, 5643.
(5) Folkes, M. J.; Keller, A. *Polymer* **1971**, *12*, 222. Folkes, M. J.; Keller, A. *J. Polym. Sci., Polym. Phys. Ed.* **1976**, *14*, 833.
(6) Archer, L. A.; Fuller, G. G.; Nunnelley, L. *Polymer* **1992**, *17*, 3574.
(7) Archer, L. A. Ph.D. Thesis, Stanford University, 1993.
(8) Archer, L. A.; Huang, K.; Fuller, G. G. Orientation dynamics of a polymer melt studied by polarization-modulated laser Raman scattering. *J. Rheol.*, in press.
(9) Long, D. A. *Raman Spectroscopy*; McGraw Hill: London, 1977.
(10) Koenig, J. L.; Coleman, M. M.; Painter, R. C. *The Theory of Vibration Spectroscopy and its Application to Polymeric Materials*; Wiley: New York, 1982. Grasselli, J. G. *Chemical Applications of Raman Spectroscopy*; Wiley: New York, 1981.
(11) Helfand, E.; Wasserman, Z. R. In *Developments in Block Copolymers-1*; Goodman, I., Ed.; Applied Science Publishers: London, 1982.
(12) Balsara, N. P.; Perahia, D.; Safinya, C. R.; Tirrell, M.; Lodge, T. P. *Macromolecules* **1992**, *25*, 3896.
(13) Keller, A.; Odell, J. A. In *Processing, Structure and Properties of Block Copolymers*; Folkes, M. J., Ed.; Elsevier: London, 1985.
(14) Inoue, T.; Okamoto, H.; Osaki, K. *Macromolecules* **1991**, *24*, 5670.
(15) Rubinstein, M.; Obukhov, S. P. *Macromolecules* **1993**, *26*, 1740.